stellarator news

Published by Fusion Energy Division, Oak Ridge National Laboratory
Building 5700 P.O. Box 2008 Oak Ridge, TN 37831-6169, USA

Editor: James A. Rome Issue 91 March 2004
E-Mail: jar@ornl.gov Phone (865) 482-5643
On the Web at http://www.ornl.gov/sci/fed/stelnews

The 10-MW ECR heating and current drive system for W7-X: First gyrotron operates at IPP-Greifswald

Electron cyclotron resonance heating (ECRH) is the main heating system for steady-state operation of W7-X (up to 30 min) in the reactor-relevant long-mean-free-path transport regime. The ECRH system for W7-X is being developed and built by the Forschungszentrum Karlsruhe (FZK) as a joint project with the Max-Planck-Institut für Plasmaphysik (IPP) and the Institut für Plasmaforschung (IPF) Stuttgart.

A heating power of 10 MW is required to meet the envisaged plasma parameters [1] at the nominal magnetic field of 2.5 T. The standard heating and current drive scenario is X2-mode with low-field-side launch. High-density operation above the X2 cut-off density at $1.2 \times 10^{20}\ m^{-3}$ will be obtained with second harmonic O-mode as well as via O-X-B mode conversion heating [2,3]. The ECRH system features a modular design consisting of ten gyrotrons (two subgroups of five gyrotrons each) at 140 GHz with 1 MW of continuous-wave (CW) output power each.

A European R&D program for the development of the W7-X gyrotron was launched in 1998 as a combined effort of several research laboratories and Thales Electron Devices (TED) as industrial partner [4]. The R&D program was successfully completed by fall 2002, demonstrating an output power of 890 kW for 180 s with an efficiency of 41% (the pulse length is limited by the FZK test stand capability for currents in excess of 25 A). The CW capability of the TED prototype gyrotron was explored at reduced beam current within the test stand limitations for CW operation (<25 A). An output power of 0.54 MW was achieved for a 15-min pulse duration at 39% efficiency. The pulse duration was then limited by internal outgassing of the gyrotron, which originated from overheating of some parts. Improved cooling will be incorporated in the production gyrotrons.

Also in 1998 and in parallel with the European R&D program, IPP placed an order with the U.S. company CPI to deliver a 140-GHz gyrotron with the same specifications. This tube passed the factory acceptance tests in early 2003. A maximum power of 910 kW was demonstrated in short-pulse operation (1–3 ms), limited by the CPI test-stand power supply. Power of 500 kW was demonstrated reliably in 600-s pulses at a reduced beam current of 26 A. Both the TED pre-prototype “Maquette” and the CPI prototype were shipped to IPP Greifswald by mid-2003 for tests with the IPP power supply, which has full-power CW capability.

Both tubes will be used to test and optimize the interplay of the required supporting systems and for integrated high-power, CW tests of the transmission system.

In this issue . . .

A quasi-optical transmission system operating at normal pressure was chosen for W7-X as a low-cost solution with high efficiency [5]. The millimeter waves are transmitted as Gaussian beams by iterative transformation with metallic mirrors. The design of such mirrors is relatively simple and straightforward. The main advantages of this technology are low ohmic and diffractive losses, high power capability due to relatively low field strength, and inherent mode filtering because high-order modes are diffracted out of the system.

The transmission line consists of single-beam waveguide (SBWG) mirror modules mounted on a common base frame and multi-beam waveguide (MBWG) mirrors for long-distance transmission. Each SBWG module is attributed to an individual gyrotron and is connected to a common water cooling circuit and equipped with a remote control unit as shown in Fig. 1.

Fig. 1. SBWG mirror module mounted in the beam duct.

Five mirrors are required for beam conditioning: Two mirrors match the Gyrotron output to a Gaussian beam with the correct beam parameters, two corrugated mirrors adjust the polarization, and one additional mirror transmits the beam to a plane mirror array, which combines the individual beams and is situated at the input plane of the MBWG (see Fig. 2). The MBWG is designed to transmit up to seven beams (five 140-GHz beams, one 70-GHz beam, plus a spare beam) from the gyrotron area (input plane) to the stellarator (output plane). At the output plane of the MBWG, a beam distribution mirror array separates the individual beams and directs each of them through a vacuum barrier window towards the plug-in launcher with the movable antennas. Four large ports of W7-X will be equipped with plug-in launchers. The total transmission efficiency of the prototype system including the diffraction due to imperfect surfaces, ohmic loss, typical misalignment, and atmospheric absorption was measured in a low-power set-up and yielded 90 ±2% for the prototype system. Good agreement with the theoretical value of 92% was found. A mode purity between 97% and 99% was deduced from amplitude and phase measurements of the various beams at the output of the MBWG.

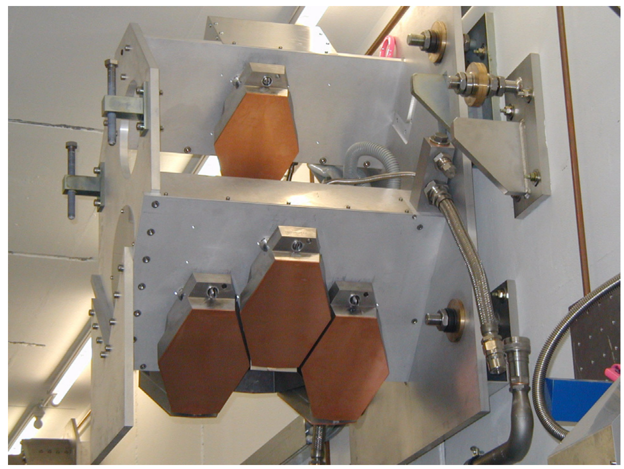

Fig. 2. Single-beam combining optics module.

The TED Maquette was successfully set into operation on 14 November 2003, demonstrating the integrated functioning of the required auxiliary systems of the ECRH plant. The gyrotron installation is shown in Fig. 3. In particular the first pre-prototype high-voltage (HV) Modulator from IPF operates reliably with the first solid-state HV power supply unit (65 kV, 50 A). Fast radio-frequency (rf) power modulation is achieved by modulating the accelerating voltage. For heat wave experiments, the gyrotrons are capable of an output power modulation between 0.3 and 1 MW with a sinusoidal frequency of up to 10 kHz. All auxiliary systems such as the gyrotron and transmission line cooling, cryogenic supply, dummy load, rf diagnostics, central control system, and network have been subject to integrated test and are now operational.

The installation of the SBWG mirror modules as well as the MBWG mirrors has been completed in the beam duct. Beam line B1, which is fed by the Maquette, was aligned, and high-power tests were started by fall 2003. During the beam alignment procedure, the remotely steerable mirror system had already proven its unique advantages and easy handling. A newly designed prototype of a short-pulse calorimeter (< 0.5 s) is installed on the SBWG frame for absolute measurement of the gyrotron output-power. The beam can be steered into a commercial CW microwave load [6] for long-pulse and CW operation (> 0.5 s). Figure 4 shows two large MBWG mirrors together with the CW loads, and the coupling mirrors.

Fig. 3. The TED Maquette gyrotron.

The CPI gyrotron and magnet are presently being installed for final full-power CW tests at IPP Greifswald. With the Maquette, the TED prototype, and the CPI tube available, seven more production-level gyrotrons are needed to complete the installation. A contract for the delivery of these tubes was placed with TED in August 2003, and a contract for the required eight additional superconducting magnets was placed with the U.S. company Cryomagnetics Inc.

The project has now entered the phase of intense tests and series installation. The ECRH team (shown in Fig. 5) had good reasons to celebrate this important milestone.

V. Erckmann for the W7-X ECRH teams at IPP,[1] FZK,[2] and IPF[3]

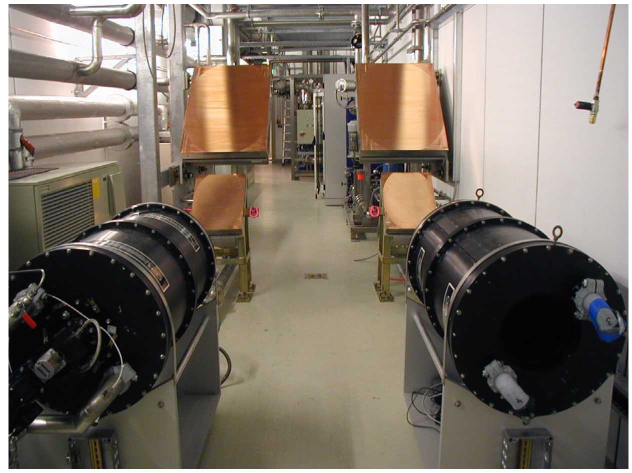

Fig. 4. Multi-beam waveguide mirrors, dummy-load coupling mirrors, and two CW Loads in the MBWG section of the beam duct.

Fig. 5. The ECRH team celebrates the first gyrotron pulse in the control room at IPP-Greifswald.

[1] Max-Planck-Institut für Plasmaphysik, Teilinstitut Greifswald, Association EURATOM,
Wendelsteinstr. 1, D-17491 Greifswald, Germany
[2] Forschungszentrum Karlsruhe, Association EURATOM-FZK, Institut für Hochleistungsimpuls und Mikrowellentechnik, Postfach 3640, D-76021 Karlsruhe, Germany,
[3] Institut für Plasmaforschung, Universität Stuttgart, Pfaffenwaldring 31, D-70569 Stuttgart, Germany

References

[1] V. Erckmann, H. J. Hartfuß, M. Kick, H. Renner, J. Sapper, F. Schauer, E. Speth, F. Wesner, F. Wagner, M. Wanner, A.Weller, and H. Wobig, "The W7-X Project: Scientific Basis and Technical Realization." pp. 40–48 in Proc. 17th IEEE/NPSS Symposium on Fusion Engineering, San Diego, USA (1997), IEEE, Piscataway, NJ, 1998.

[2] V. Erckmann and U. Gasparino, "Electron cylotron resonance heating and current drive in toroidal fusion plasmas," Plasma Phys. Controlled Fusion **36** (1994) 1869–1962.

[3] H. P. Laqua, V. Erckmann, H. J. Hartfuß, H. Laqua,W7-AS Team, and ECRH Group, "Resonant and nonresonant Electron Cyclotron Heating at Densities above the Plasma Cut off by O-X-B Mode Conversion at the W7-AS Stellarator," Phys. Rev. Lett. **78** (1997) 3467.

[4] G. Dammertz, et al. IEEE Trans. Plasma Sci. **30** (2002) 808–818.

[5] L. Empacher, W. Förster, G. Gantenbein, W. Kasparek, G. A. Müller, P. G. Schüller, K. Schwörer, U. Schumacher, D. Wagner, V. Erckmann, T. Geist, and H. Laqua, "Conceptual Design of the 140 GHz / 10-MW CW ECRH System for the Stellarator W7-X," pp. 541–544 in Fusion Technology 1996, Elsevier Science B.V., Amsterdam 1997.

[6] R.L. Ives et al.,"Development of a 1 MW CW Waterload for Gaussian Mode Gyrotrons," pp. 226–227 in Conf. Digest, 23rd Int. Conf. Infrared Millimeter Waves, Colchester (UK), 1998.

Effects of global MHD instabilities on the operational high-beta regime in LHD

A helical device is a promising candidate for the toroidal magnetic confinement system of a steady-state thermonuclear fusion reactor. Since the heliotron configuration has a magnetic hill in the peripheral region, magnetohydrodynamic (MHD) stability theory suggests that pressure-driven MHD instabilities such as interchange modes are a concern in the high-beta regime. Therefore, understanding and controlling pressure-driven modes in the high-beta regime is one of the critical issues for a helical fusion reactor. Recent progress in heating capability in the Large Helical Device (LHD) [1] enables exploration of MHD studies in the beta range $\beta > 3\%$. In order to evaluate the effects of global ideal MHD modes on the operational regime in LHD, we compare the experimentally achieved pressure gradient at resonant rational surfaces and the theoretical prediction.

A limited amount of experimental research on the effect of interchange modes on the operational regime in heliotron devices has been conducted, for example, on Heliotron DR [2] and the Compact Helical System (CHS) [3]. The results of these works differ. In Heliotron-DR, the experimentally achieved beta is consistent with the theoretically estimated beta limit given by low-*n* ideal interchange instabilities. In contrast, discharges are maintained in the unstable region predicted by low-*n* ideal MHD stability calculations in CHS. In the previous works, attention was generally paid to the average beta, and not particularly to the pressure profile, in studying the operational regime.

The stability of interchange modes depends on the pressure gradients at resonant rational surfaces. Moreover, the pressure gradient and any net toroidal current affect the stability of interchange modes through the change of MHD equilibrium at finite beta, for example, the Shafranov shift, magnetic well formation, and so on. This type of change in MHD equilibrium becomes significant in devices with low aspect ratio and/or low rotational transform, such as CHS and LHD. In order to clarify the role of interchange instabilities on the operational regime, it is necessary to analyze the relationship between the unstable condition of the interchange modes and the experimentally observed pressure gradients at every resonant rational surface based on an MHD equilibrium that is consistent with measured data such as density, temperature, and plasma current. LHD has very capable systems to measure profiles; for example, electron profiles are measured at more than 100 positions by Thomson scattering [4], which enables detailed comparative analysis of experiment and calculation.

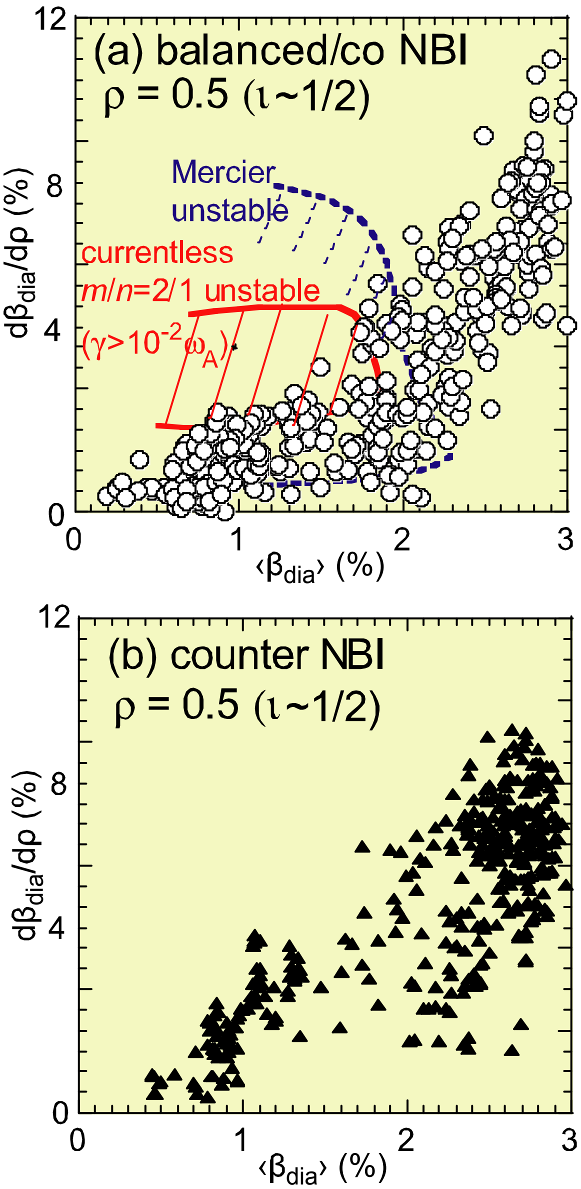

Fig. 1. Pressure gradients achieved experimentally at ρ = 0.5 (core) in R_{ax} = 3.6 m configuration in $\langle\beta\rangle$–$d\beta/d\rho$ space with (a) co- and balanced NBI and (b) counter-NBI.

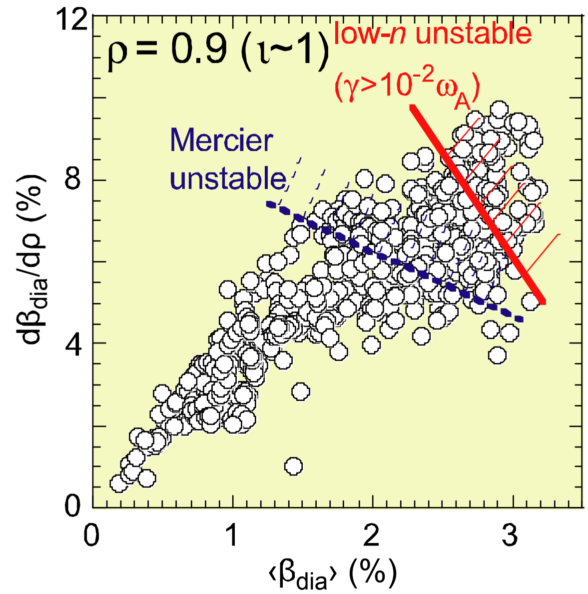

Fig. 2. Pressure gradients achieved experimentally at ρ = 0.9 (edge) in R_{ax} = 3.6 m configuration in $\langle\beta\rangle$–$d\beta/d\rho$ space.

Figures 1 and 2 show the experimentally observed pressure gradients $d\beta_{dia}/d\rho$ at ρ = 0.5 and 0.9 versus $\langle\beta_{dia}\rangle$ in the R_{ax} = 3.6 m configuration with magnetic fields in the range 0.5–1.5 T. Here β_{dia} is based on diamagnetic flux measurements, angle brackets $\langle\ \rangle$ denote a volume-averaged value, and the beta profile is assumed to be proportional to the electron pressure, which is the product of the electron temperature obtained from the Thomson scattering measurement and the electron density from a far-infrared (FIR) interferometer measurement. Note that rational surfaces with rotational transforms of 1/2 and 1/1 are located near ρ = 0.5 and ρ = 0.9, respectively.

According to measurements of the magnetic fluctuations, a resonant fluctuation in the core (m/n = 2/1) is observed in the range 0.3% < $\langle\beta_{dia}\rangle$ < 2.3%, which coincides with the Mercier unstable region. The resonant fluctuation in the edge (m/n = 1/1) is observed for all beta values below $\langle\beta_{dia}\rangle$ ~ 3% [5]. Here m and n are the toroidal and poloidal mode numbers, respectively. Solid and dashed lines in Figs. 1 and 2 denote the stability boundaries for low-n (m/n = 2/1, 1/1) ideal modes (global modes) and Mercier modes (highly localized modes), respectively, for currentless equilibria.

The stability of low-n ideal MHD modes is calculated by using a three-dimensional (3D) MHD stability analyzing code (TERPSICHORE [6]) for various pressure profiles. Here, we define a contour of the growth rate, $\gamma_{low\text{-}n} = 10^{-2}\omega_A$ (ω_A is the Alfvén frequency), as the stability boundary, which corresponds to the Mercier parameter, D_I

~ 0.3. Circles in Fig. 1(a) correspond to the observed pressure gradients under co- and balanced neutral beam injection (NBI). The experimentally observed pressure gradients seem to saturate against the contour of $\gamma_{\text{low-}n} = 1.5 \times 10^{-2}\ \omega_A$. This value exceeds the stability boundary defined here, which corresponds to a contour of the growth rate of low-*n* ideal MHD mode estimated by TERPSICHORE, namely $\gamma_{\text{low-}n} = 1.5 \times 10^{-2}\ \omega_A$. When $\langle\beta_{dia}\rangle$ exceeds ~1.8%, the maximum achieved pressure gradient more than doubles.

These experimental observations coincide with violation of low-*n* modes and stabilization due to spontaneous generation of a magnetic well resulting from the Shafranov shift. Triangles in Fig. 1(b) correspond to the observed pressure gradients under counter-NBI. Counter-NBI discharges tend to induce negative Ohkawa currents in the core and positive bootstrap currents in the periphery, which reduce the Shafranov shift at the edge and enhance it in the core. Consequently, these induced currents are expected to lead to a deeper magnetic well and larger magnetic shear in the core than those in the cases of co- and balanced NBI discharges. When we assume a current profile model with negative currents in the core and positive currents in the periphery, consistent with experimental conditions, the theoretically predicted unstable region disappears in $\langle\beta\rangle$–$d\beta/d\rho$ space. The experimentally achieved pressure gradients in the case with counter-NBI exceed the upper bound of those in the case with co- and balanced NBI below $\langle\beta_{dia}\rangle$ ~ 1.8%. These experimental results suggest that the low-*n* ideal MHD modes limit the operational regime through the pressure gradient limit in the core region in LHD experiments. In Fig. 2, the achieved pressure gradients at $\rho = 0.9$ exhibit a slight saturation with the increase in $\langle\beta_{dia}\rangle$. However, the achieved pressure gradients at $\rho = 0.9$ occur deeper into the low-*n* mode (*m*/*n*=1/1) unstable region than is the case in the core.

Figure 3 shows the improvement factor (H_{ISS}) in the International Stellarator Scaling 1995 (ISS95) global energy confinement empirical scaling [7] as a function of $\langle\beta_{dia}\rangle$. Here H_{ISS} is also based on the diamagnetic flux measurements. All data correspond to only NBI-heated and H_2 gas-fueled discharges. In low-field operation, the heating efficiency strongly depends on the magnetic field strength. High-beta operations below $B_0 = 0.4$ T in LHD are difficult because of the poor confinement properties of fast ions created by NBI. Above $\langle\beta_{dia}\rangle$ ~ 3%, data lie between 1 and 1.5 and a slight degradation of the global energy confinement time with increasing beta is observed. However, in this range of $\langle\beta_{dia}\rangle$, we have not yet found any significant degradation of beta.

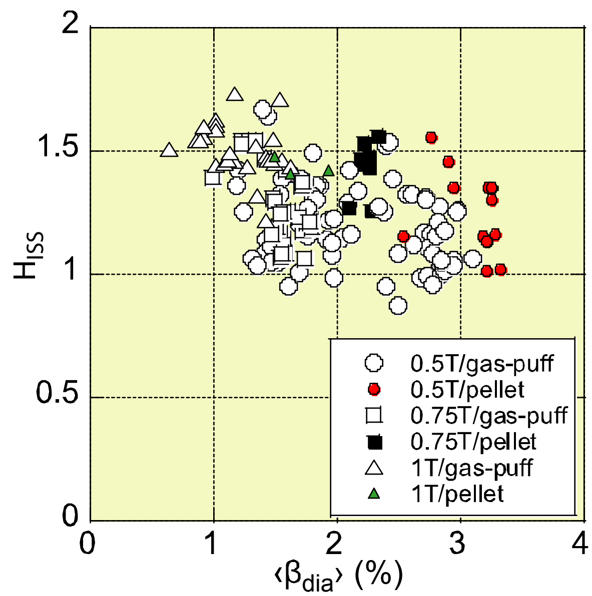

Fig. 3. The improvement factor of effective energy confinement in relatively low-field discharges.

In order to clarify whether global ideal MHD modes limit the pressure gradients in the edge as they do in the core, we should take into account the results of local transport analysis, and the comparison of theoretical predictions and the observed pressure gradients could be extended to other magnetic configurations in LHD. These are our important future subjects.

K.Y.Watanabe and LHD Experimental Group
National Institute for Fusion Science
322-6 Oroshi, Toki, 509-5292, Japan
E-mail: kiyowata@LHD.nifs.ac.jp

References

[1] O. Motojima et al., Nucl. Fusion **43**, 1674 (2003).
[2] N. Yanagi et al., Nucl. Fusion **32**, 1264 (1989).
[3] S. Okamura et al., Nucl. Fusion **30**, 1337 (1999).
[4] K. Narihara et al., Rev. Sci. Instrum. **72**, 1122 (2001).
[5] S. Sakakibara et al., Plasma Phys. Control. Fusion **44**, A217 (2002).
[6] W. A. Cooper, Plasma Phys. Controlled Fusion **34**, 1011 (1992).
[7] U. Stroth et al., Nucl. Fusion **36**, 1063 (1996).